Plasmonic hot spots: nanogap enhancement vs. focusing effects from surrounding nanoparticles

Prathamesh Pavaskar, Jesse Theiss and Stephen B. Cronin*

Ming Hsieh Department of Electrical Engineering, University of Southern California, Los Angeles, California 90089, USA

*scronin@usc.edu

Abstract: Thin Au films (~5nm) are known to form island-like structures with small gaps between the islands, which produce intense electric field "hot spots" under visible illumination. In this work, we perform finite difference time domain (FDTD) simulations based on experimentally observed high resolution transmission electron microscope (HRTEM) images of these films in order to study the nature of the "hot spots" in more detail. Specifically, we study the dependence of the electric field intensity in the hot spots on the surrounding film environment and on the size of the nanogaps. From our simulations, we show that the surrounding film contributes significantly to the electric field intensity at the hot spot by focusing energy to it. Widening of the gap size causes a decrease in the intensity at the hot spot. However, these island-like nanoparticle hot spots are far less sensitive to gap size than nanoparticle dimer geometries, studied previously. In fact, the main factor in determining the hot spot intensity is the focusing effect of the surrounding nano-islands. We show that these random Au island films outperform more sophisticated geometries of spherical nanoparticle clusters that have been optimized using an iterative optimization algorithm.

OCIS codes: (240.6680) Surface plasmons; (260.3910) Metal optics.

References and links

1. K. Kneipp, H. Kneipp, P. Corio, S. D. M. Brown, K. Shafer, J. Motz, L. T. Perelman, E. B. Hanlon, A. Marucci, G. Dresselhaus, and M. S. Dresselhaus, "Surface-enhanced and normal stokes and anti-stokes Raman spectroscopy of single-walled carbon nanotubes," Phys. Rev. Lett. **84**(15), 3470–3473 (2000).
2. P. Corio, S. D. M. Brown, A. Marucci, M. A. Pimenta, K. Kneipp, G. Dresselhaus, and M. S. Dresselhaus, "Surface-enhanced resonant Raman spectroscopy of single-wall carbon nanotubes adsorbed on silver and gold surfaces," Phys. Rev. B **61**(19), 13202–13211 (2000).
3. W. Hou, W. H. Hung, P. Pavaskar, A. Goeppert, M. Aykol, and S. B. Cronin, "Photocatalytic Conversion of CO_2 to Hydrocarbon Fuels via Plasmon-Enhanced Absorption and Metallic Interband Transitions," J. Am. Chem. Soc. **1**(8), 929–936 (2011).
4. W. Hou, Z. Liu, P. Pavaskar, W. H. Hung, and S. B. Cronin, "Plasmonic Enhancement of Photocatalytic Decomposition of Methyl Orange under Visible Light," J. Catal. **277**(2), 149–153 (2011).
5. Z. Liu, W. Hou, P. Pavaskar, M. Aykol, and S. B. Cronin, "Plasmon resonant enhancement of photocatalytic water splitting under visible illumination," Nano Lett. **11**(3), 1111–1116 (2011).
6. G. Kalyuzhny, A. Vaskevich, G. Ashkenasy, A. Shanzer, and I. Rubinstein, "UV/Vis spectroscopy of metalloporphyrin and metallophthalocyanine monolayers self-assembled on ultrathin gold films," J. Phys. Chem. B **104**(34), 8238–8244 (2000).
7. G. Kalyuzhny, A. Vaskevich, M. A. Schneeweiss, and I. Rubinstein, "Transmission surface-plasmon resonance (T-SPR) measurements for monitoring adsorption on ultrathin gold island films," Chemistry **8**(17), 3849–3857 (2002).
8. I. Tokareva, S. Minko, J. H. Fendler, and E. Hutter, "Nanosensors based on responsive polymer brushes and gold nanoparticle enhanced transmission surface plasmon resonance spectroscopy," J. Am. Chem. Soc. **126**(49), 15950–15951 (2004).
9. R. P. Van Duyne, J. C. Hulteen, and D. A. Treichel, "Atomic force microscopy and surface-enhanced Raman spectroscopy. I. Ag island films and Ag film over polymer nanosphere surfaces supported on glass," J. Chem. Phys. **99**(3), 2101 (1993).

#167595 - $15.00 USD Received 27 Apr 2012; revised 30 May 2012; accepted 31 May 2012; published 15 Jun 2012

10. P. Royer, J. P. Goudonnet, R. J. Warmack, and T. L. Ferrell, "Substrate effects on surface-plasmon spectra in metal-island films," Phys. Rev. B Condens. Matter **35**(8), 3753–3759 (1987).
11. F. Brouers, S. Blacher, A. N. Lagarkov, A. K. Sarychev, P. Gadenne, and V. M. Shalaev, "Theory of giant Raman scattering from semicontinuous metal films," Phys. Rev. B **55**(19), 13234–13245 (1997).
12. F. Brouers, S. Blacher, and A. K. Sarychev, "Giant field fluctuations and anomalous light scattering from semicontinuous metal films," Phys. Rev. B **581**, 1411451–1415903 (1998).
13. U. K. Chettiar, P. Nyga, M. D. Thoreson, A. V. Kildishev, V. P. Drachev, and V. M. Shalaev, "FDTD modeling of realistic semicontinuous metal films," Appl. Phys. B **100**(1), 159–168 (2010).
14. S. Gresillon, L. Aigouy, A. C. Boccara, J. C. Rivoal, X. Quelin, C. Desmarest, P. Gadenne, V. A. Shubin, A. K. Sarychev, and V. M. Shalaev, "Experimental observation of localized optical excitations in random metal-dielectric films," Phys. Rev. Lett. **82**(22), 4520–4523 (1999).
15. S. Ducourtieux, V. A. Podolskiy, S. Grésillon, S. Buil, B. Berini, P. Gadenne, A. C. Boccara, J. C. Rivoal, W. D. Bragg, K. Banerjee, V. Safonov, V. Drachev, Z. Ying, A. Sarychev, and V. Shalaev, "Near-field optical studies of semicontinuous metal films," Phys. Rev. B **64**(16), 165403 (2001).
16. J. Theiss, P. Pavaskar, P. M. Echternach, R. E. Muller, and S. B. Cronin, "Plasmonic nanoparticle arrays with nanometer separation for high-performance SERS substrates," Nano Lett. **10**(8), 2749–2754 (2010).
17. E. Hao and G. C. Schatz, "Electromagnetic fields around silver nanoparticles and dimers," J. Chem. Phys. **120**(1), 357–366 (2004).
18. C. Oubre and P. Nordlander, "Finite-difference time-domain studies of the optical properties of nanoshell dimers," J. Phys. Chem. B **109**(20), 10042–10051 (2005).
19. S. Palomba, M. Danckwerts, and L. Novotny, "Nonlinear plasmonics with gold nanoparticle antennas," J. Opt. A, Pure Appl. Opt. **11**(11), 114030 (2009).
20. A. Taflove and S. C. Hagness, *Computational electrodynamics* (Artech House, 1995).
21. E. D. Palik and G. Ghosh, *Handbook of optical constants of solids* (Academic Press, 1998).
22. K. H. Su, Q. H. Wei, X. Zhang, J. J. Mock, D. R. Smith, and S. Schultz, "Interparticle coupling effects on plasmon resonances of nanogold particles," Nano Lett. **3**(8), 1087–1090 (2003).
23. T. Atay, J. H. Song, and A. V. Nurmikko, "Strongly interacting plasmon nanoparticle pairs: From dipole-dipole interaction to conductively coupled regime," Nano Lett. **4**(9), 1627–1631 (2004).
24. J. Aizpurua, G. W. Bryant, L. J. Richter, F. J. G. De Abajo, B. K. Kelley, and T. Mallouk, "Optical properties of coupled metallic nanorods for field-enhanced spectroscopy," Phys. Rev. B **71**(23), 235420 (2005).
25. P. Pavaskar and S. B. Cronin, "Iterative optimization of plasmon resonant nanostructures," Appl. Phys. Lett. **94**(25), 253102 (2009).

1. Introduction

It is well known that thin films (~ 5nm) of noble metals such as Au and Ag exhibit a strong plasmonic response under visible illumination due to their discontinuous nature. These thin plasmonic films have been used in surface enhanced Raman spectroscopy (SERS) [1,2], plasmon-enhanced photocatalysis [3–5], and sensing applications [6–8]. Van Duyne *et al.* showed that the island-like structure of these films facilitates large enhancement in electric fields [9]. Royer *et al.* studied the structure of 5nm thick Au and Ag films using scanning electron microscope (SEM) and approximated the shape of the film islands using oblate spheroids in order to perform theoretical calculations [10]. These island-like structures create localized "hot spot" regions, in which the local electric field intensity can be enhanced by several orders of magnitude [11]. The Purdue group has studied these hot spot thin films both theoretically [11–13] and experimentally [14,15]. The general consensus is that these hot spots tend to form in regions where the neighboring islands are nearly touching, allowing for maximum plasmonic coupling. This has been observed in the case of nanoparticle dimers as well [16–19].

#167595 - $15.00 USD Received 27 Apr 2012; revised 30 May 2012; accepted 31 May 2012; published 15 Jun 2012

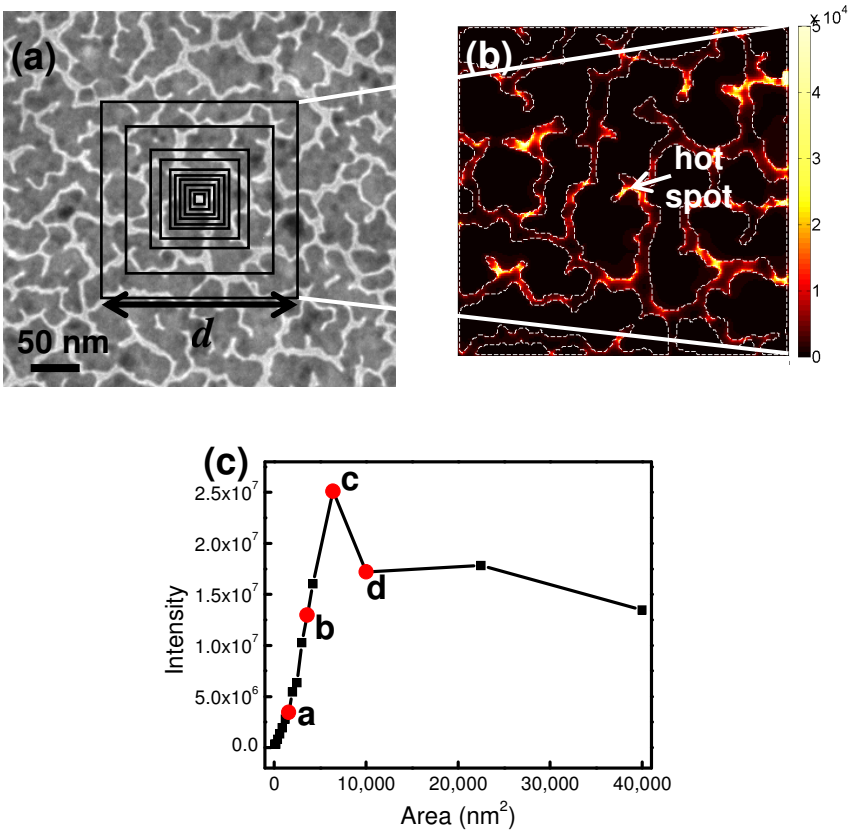

Fig. 1. (a) HRTEM micrograph and (b) electric field profile of the region surrounding a hot spot on a 5nm Au island film. The black squares of area (*d* x *d*) in (a) correspond to the different film areas used in the simulations shown in (c). (c) Electric field intensity at the hot spot plotted as a function of area (*d* x *d*).

We believe that the electric field enhancement in these hot spots, apart from being dependent on the gap size between the islands, is also influenced by the surrounding nanoparticles in the film. In this paper, we study the effect of the surrounding environment on the local electric field at the hot spot. Specifically, we determine how much of the electric field at the hot spot is contributed by the focusing effect of the surrounding film. To achieve this, we performed finite difference time domain (FDTD) simulations [20] of several hot spots based on experimentally measured high resolution transmission electron microscope (HRTEM) images of 5nm Au films and systematically varied the nano-island and gap size.

2. Simulation details

Au films were deposited on 100nm thick SiN membranes by electron-beam evaporation to achieve a nominal thickness of 5nm, as determined by a quartz crystal oscillator thickness monitor. HRTEM images were taken in a JEOL JEM-2100F advanced field emission transmission electron microscope, which provides high contrast images of the Au island films with <2Å resolution. These images were then used to define the spatial extent of the Au islands in the electromagnetic simulations. The thickness of the Au islands for the simulations was chosen to be 5nm. We neglected the surface roughness of the film, as the significant electric fields are present in the gaps between the islands and not on the surface of the islands. Full three-dimensional FDTD simulations were carried out on the University of Southern California's 0.15 petaflop supercomputing facility, which consists of 14,734 CPUs connected

#167595 - $15.00 USD Received 27 Apr 2012; revised 30 May 2012; accepted 31 May 2012; published 15 Jun 2012

by a high-performance, low-latency Myrinet network. A simulation cell size of 600nm x 600nm x 500nm was used with a grid spacing of 2Å in the volume of 200 x 200 x 20nm^3 around the film. 100,000 discrete time steps with a temporal grid spacing of 0.002 fsec were used in these calculations. A normal incidence, Gaussian pulse planewave source was used in the simulations with a broad spectrum of wavelengths ranging from 500nm to 1100nm. Perfectly matched layers (PML) were used as boundary conditions with 64 layers. The dielectric function of Au was a Lorentz-Drude model fitted to the optical data given by Palik and Ghosh. A uniform mesh was used over the entire simulation volume [21].

3. Results and discussion

Figure 1(a) shows a high resolution TEM image of a 5nm nominal Au film centered on a hot spot. Figure 1(b) shows the simulated electric field profile of the selected region. We performed several simulations on this hot spot, selectively removing the metal material around the hot spot and replacing it by vacuum. This scheme is illustrated more clearly in Fig. 2. The black squares of area (d x d) in Fig. 1(a) show the different film regions used in these simulations. We, thus, limit the total size of the film to an area of (d x d), while keeping the simulation area and mesh constant, to avoid any unphysical factors that may influence the results of the simulation. The electric field intensity at the centermost hot spot, I, was calculated by integrating the square of the electric field intensity over a 10 x 10 x 15nm^3 volume centered on the hot spot region and over all wavelengths. The integral in the z-dimension is centered on the Au-SiN interface. Thus, I is calculated as

$$I = \int_{500nm}^{1100nm} d\lambda \iiint dxdydz \, |E(x, y, z, \lambda)|^2$$

The electric field intensity integrated over a small volume provides a more reliable value than the intensity at a point, by minimizing the effects that may arise due to sharp features artificially created by the spatial discretization. The hot spot intensity calculated in this manner is plotted as a function of plasmonic film area in Fig. 1(c). In this plot, the intensity increases with area initially, but drops beyond 6400nm^2 (i.e., 80nm x 80nm). The surrounding film is, therefore contributing energy to the local hot spot causing this initially increasing trend. It should be noted that the integrated intensity, I, is different than the electric field intensity shown in Fig. 1(b).

Similar results were observed for several such hot spots. In order to fully understand the drop in intensity for larger areas, we plot the electric field intensity profiles of several different areas in Fig. 2. The electric field profiles shown in Fig. 2(a) to Fig. 2(d) correspond to the highlighted data points shown in Fig. 1(c). Figures 2(a) to 2(c) clearly show that the hot spot at the center is the dominant hot spot, and there is a monotonic increase in the hot spot intensity with area. However, the electric field profile shown in Fig. 2(d) shows the presence of an additional hot spot that is more dominant than the one at the center. The new dominant hot spot is indicated by the arrow in Fig. 2(d). The intensity drop from 6400nm^2 (80nm x 80nm) to 10,000nm^2 (100nm x 100nm) can, therefore, be explained by the presence of the additional hot spot, which takes energy from the centermost hot spot. We also notice another hot spot appearing and disappearing as the area is increased. This phenomenon can be attributed to the fact that, the addition of the surrounding nanoparticles focuses light to a given hot spot by varying degrees, depending on their specific morphology.

We also study the effect of widening the gap of a hot spot on the electric field intensity by artificially removing metal from the hot spot region, thus reducing the gap size. Figure 3(b) shows the relation between the hot spot intensity and gap size. As expected, the intensity at the centermost hot spot (labeled HS_0 in Fig. 3(a)) decreases with gap size, due to the decreased coupling between plasmons across the gap. This effect has been reported both theoretically and experimentally in the case of plasmonic nanoparticle pairs [17,22,23]. The

#167595 - $15.00 USD Received 27 Apr 2012; revised 30 May 2012; accepted 31 May 2012; published 15 Jun 2012

intensities of the other two hot spots (HS_1 and HS_2), however, remain mostly unaffected as the gap size of the central hot spot HS_0 is changed.

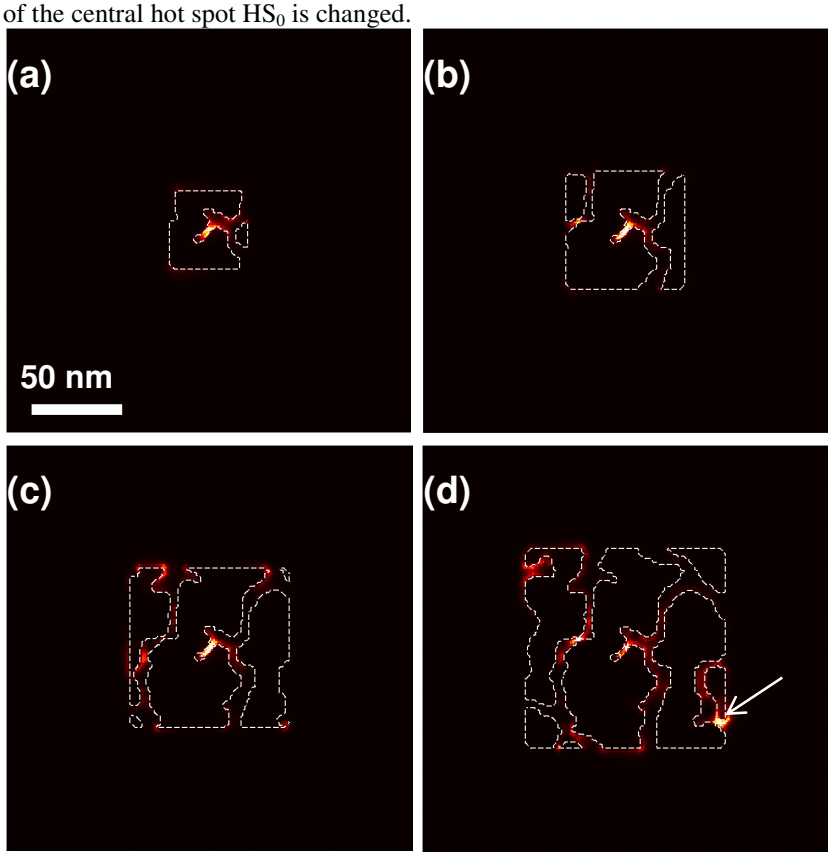

Fig. 2. Electric field intensity profiles corresponding to the areas highlighted in Fig. 1(c).

The monotonic decrease in the hot spot intensity as the gap size is increased shows that there is plasmonic coupling between the islands across the gap. However, the rate of decrease in the intensity is not as high as in the case of nanoparticle dimers [17,24], which show an exponential decrease in the electric field intensity when the gap size is increased. Hao and Schatz reported a 10-fold decrease in the electric field intensity with only a 2nm increase in the gap size [17]. Aizpurua *et al*. showed a 25-30X drop in the electric field intensity when the gap size is changed from 2nm to 10nm [24]. However, in our case, there is only a 2.6X decrease in the intensity when the gap is increased from 2nm to 10nm. Thus, these island-like nanoparticle hot spots are more robust to changes in the gap size than the corresponding spherical or cylindrical nanoparticle geometries. This is due to the significant contribution made by the surrounding metal islands to the hot spot intensity, as shown in Fig. 1 and Fig. 2. This has important implications on the future design of nanoparticle arrays for optimized plasmonic hot spot applications. It should be noted that widening the gap of a hot spot only changes the plasmonic coupling locally and thus should not affect the surrounding hot spots in any way, if the area of the film (d x d) is held constant, as seen in Fig. 3(b).

#167595 - $15.00 USD Received 27 Apr 2012; revised 30 May 2012; accepted 31 May 2012; published 15 Jun 2012

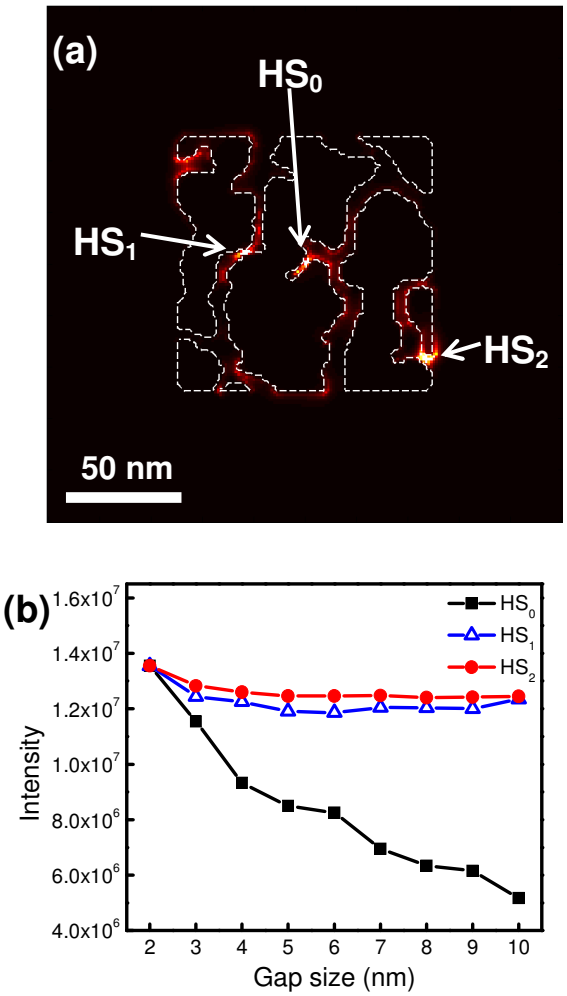

Fig. 3. (a) Electric field intensity profile of a region with 3 hot spots labeled HS_0, HS_1 and HS_2. (b) Electric field intensities of HS_0, HS_1 and HS_2 plotted as a function of the HS_0 gap size.

In our previous work, the geometries of nanoparticle clusters giving the maximum electric field intensity at the center of the cluster was determined using an iterative optimization algorithm [25]. Here, the surrounding nanoparticles in the cluster focus light on the central hot spot. This previous work, was carried out using 2D FDTD simulations for light incident in the plane of the nanoparticle cluster. More recently, we have carried out full 3D FDTD simulations of nanoparticle clusters under normal incidence illumination. Figure 4 shows the electric field intensity plot for the optimum configuration of a 20-nanoparticle cluster. This nanoparticle configuration was the result of an iterative optimization scheme with respect to 40 dimensions (i.e., x and y positions of 20 nanoparticles). In order to obtain this geometry, we started with a cluster of two nanoparticles and performed the optimization routine for the position of a third nanoparticle. The position of each additional nanoparticle was optimized using this scheme up to a total of 20 nanoparticles each having a diameter of 40nm. Adding more nanoparticles would have increased the computational cost while not providing any further insight into plasmonic optimization, since the resulting geometries were highly symmetric. Additionally, the overall size of this cluster geometry is of the same order as that of the largest film area we used in our simulations. These calculations were performed using 16 processors in parallel, and altogether they took approximately 1700 hours. Despite the

#167595 - $15.00 USD Received 27 Apr 2012; revised 30 May 2012; accepted 31 May 2012; published 15 Jun 2012

relative computational intensity of this calculation, the resulting optimized nanoparticle cluster only produces an integrated electric field intensity, *I*, of 10^6 at the centermost hot spot. This is more than an order of magnitude smaller than the integrated electric field intensity observed in the randomly-shaped Au island films of comparable size. The main reason for the relatively poor performance of the optimized nanoparticle cluster is that it contains many hot spots, which all compete for energy from the same incident electromagnetic flux. This will be an important consideration in future efforts to design and optimize plasmonic hot spot nanostructures, which has not yet been taken into account. It is likely that more intense hot spots that make more efficient use of the available surface area are possible by considering the focusing effects associated with arbitrary shaped geometries. Again, we would like to point out that the quantity plotted in figure 4 is the electric field intensity, which is different than the integrated intensity, *I*.

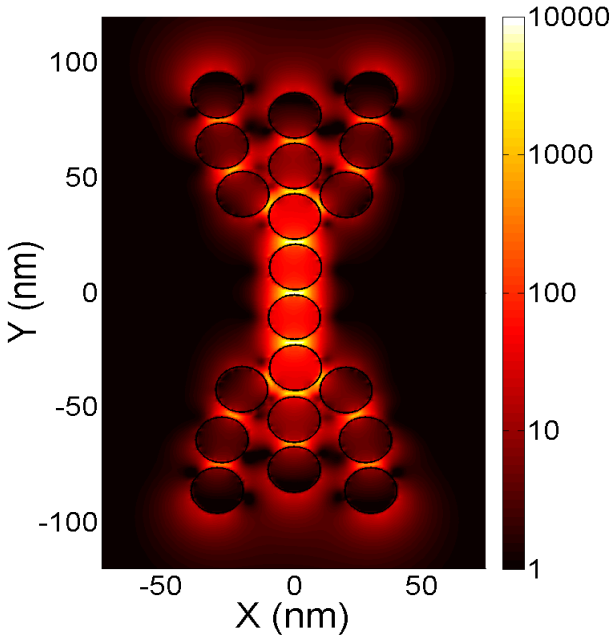

Fig. 4. Electric field intensity profile for an optimized cluster of 20 nanoparticles.

4. Conclusions

In conclusion, we have studied the dependence of nanogap "hot spots" in thin plasmonic films on the presence of surrounding nano-islands. FDTD simulations demonstrate that the surrounding film environment contribute significantly to the intensity at the hot spot by focusing energy to it. However, the presence of other dominant hot spots in the surrounding film can take energy away from the central hot spot. We have shown that widening of the gap size causes a decrease in the intensity at the hot spot, while the surrounding hot spots remain unaffected. However, these island-like nanoparticle hot spots are far less sensitive to gap size than nanoparticle dimer geometries. In fact, the main factor in determining the hot spot intensity is the focusing effect of the surrounding nano-islands. In the future design of plasmonic nanostructures, this focusing effect will be an important consideration in producing optimized plasmonic films.

Acknowledgments

This research was supported by AFOSR Award No. FA9550-08-1-00190019 and ONR Award No. N00014-12-1-0570.

#167595 - $15.00 USD Received 27 Apr 2012; revised 30 May 2012; accepted 31 May 2012; published 15 Jun 2012